Photochemical & Photobiological Sciences

Accepted Manuscript

This is an *Accepted Manuscript*, which has been through the Royal Society of Chemistry peer review process and has been accepted for publication.

Accepted Manuscripts are published online shortly after acceptance, before technical editing, formatting and proof reading. Using this free service, authors can make their results available to the community, in citable form, before we publish the edited article. We will replace this *Accepted Manuscript* with the edited and formatted *Advance Article* as soon as it is available.

You can find more information about *Accepted Manuscripts* in the Information for Authors.

Please note that technical editing may introduce minor changes to the text and/or graphics, which may alter content. The journal's standard Terms & Conditions and the Ethical guidelines still apply. In no event shall the Royal Society of Chemistry be held responsible for any errors or omissions in this *Accepted Manuscript* or any consequences arising from the use of any information it contains.

ROYAL SOCIETY OF CHEMISTRY

www.rsc.org/pps

Journal Name

ARTICLE

Enhanced photocatalytic bacteriostatic activity of *Escherichia coli* using 3D hierarchical microsphere BiOI/BiOBr under visible light irradiation

Received 00th January 20xx,
Accepted 00th January 20xx

DOI: 10.1039/x0xx00000x

www.rsc.org/

Ya Wang,[a] Li Lin,[a] Fang Li, [a] Liang Chen,[a*] Donghui Chen,[b] Chongyang Yang,[a] and Manhong Huang,[a*]

The BiOI/BiOBr composite was successfully fabricated by a simple hydrothermal method. The composite was characterized by X-ray diffraction (XRD), UV–vis diffuse reflectance spectrum (UV–vis DRS), scanning electron microscopy (SEM), high-resolution transmission electron microscopy (HRTEM). The BiOI/BiOBr composite exhibited enhanced photocatalytic bacteriostatic activity of E. coli as compared to the pure BiOI or BiOBr under visible light irradiation. The enhanced photocatalytic performance can be attributed to the improved separation efficiency of the photogenerated holes because of its heterojunction structure. In addition, the possible bacteriostatic mechanism of the BiOI/BiOBr composite under visible light irradiation was discussed. The hierarchical microsphere BiOI/BiOBr showed enhanced photocatalytic bacteriostasis of Escherichia coli under visible light irradiation.

Introduction

The pathogenic microorganisms in drinking water are terribly harmful to the human health, which arouse an increasing concern all through the world [1, 2]. Although traditional chemical oxidation disinfection technologies are effective to control the microorganisms such as chlorination and ozonation, they usually produce harmful by-products with carcinogenic and mutagenic potential [3], which provides an unpredictable health hazard. Since the earliest example of the semiconductor photocatalyst TiO_2 applied as disinfection method was reported by Matsunaga et al. firstly [4], there has been a growing interest in the exploitation of photocatalytic disinfection for water in recent years. However, TiO_2 that was used most widely is only activated under UV light irradiation (about 4% sunlight), which greatly limits the utilization of solar irradiation. Therefore, developing high performance and no-toxic photocatalysts with good visible light response for water disinfection is necessary since 45% of the sunlight spectrum is visible light [5].

Due to the unique optical properties and their promising industrial applications, Bismuth oxyhalides, BiOX (X = Cl, Br, I), have been extensively investigated in recent years [6-9]. Besides, Bismuth (Bi), which is a kind of p-block metal with a d10 configuration, can narrow the band gap because of the hybridized valence band by O 2p and Bi 6s. And it can accelerate the mobility of photo-generated holes in the visible light [10, 11]. Recent studies about the BiOX mainly focus on the degradation of organic pollutants and rather few in water disinfection [12, 13]. Moreover, semiconductor heterogeneous photocatalysis is considered as a promising alternative way for disinfection. In order to improve the charge-transfer efficiency of single semiconductor, the synthesis of composite materials with a heterojunction structure has become an area of growing interest. For example, Gan et al. [14] reported the $Bi_2O_2CO_3/Bi_3NbO_7$ heterojunction enhanced visible-light-driven photocatalytic inactivation of *Escherichia coli.* In composite semiconductor materials, the heterostructures are constructed between the semiconductors with matching band potentials. Thus, feasible photo-generated electrons and/or holes transfer from one semiconductor to another can greatly inhibit the electrons and holes recombination, increase the lifetime of charge carriers, and improve the photocatalytic efficiency [14, 15]. Several hybrids of two or more semiconductor systems have been reported, e.g., BiOBr/BiOI [16], BiOI/BiOCl [17] AgI/BiOI [18], WO_3/BiOCl [19], $Bi_2WO_6/ZnWO_4$ [20], etc., and proven to be efficient in photocatalytic degrading organic pollutants. Dong et al. reported BiOI/BiOCl[21] and $BiOIO_3$/BiOI[22] heterostructures showed highly enhanced visible photocatalytic performance for NO removal. Furthermore, BiOI/AgI [23] $Bi_2O_2CO_3/Bi_3NbO_7$ composites [14], $In_2O_3/CaIn_2O_4$ photocatalyst [24] and ZnO/SnO_2 heterojunction [25] were reported to have enhanced bactericidal property.

Herein, we synthesized the 3D hierarchical microsphere BiOI/BiOBr with heterojunction structures by a one-pot solvothermal method easily and investigated the photocatalytic bacteriostatic performance of bacteria using the composite under visible light. In standards for disinfection

[a] College of Environmental Science and Engineering, State Environmental Protection Engineering Center for Pollution Treatment and Control in Textile Industry, Donghua University, Shanghai 201620, China
[b] School of Chemical and Environmental Engineering, Shanghai Institute of Technology, Shanghai 200235, China.
*Corresponding Authors e-mail:egghmh@163.com;chliang@dhu.edu.cn

under visible light, *E.coli* was used as a typical strain of intestinal bacteria.

Experimental

Synthesis of photocatalysts

In the experiment, all chemical reagents with analytical grade were used without further purification and purchased from the Sinopharm Chemical Reagent Co.Ltd., China (Shanghai, China). The BiOI, BiOBr and BiOI/BiOBr composites were all synthesized by the one-pot solvothermal approach. Firstly, $Bi(NO_3)_3 \cdot 5H_2O$ (2.8 mmol) and poly vinyl pyrrolidone (PVP) (0.15 g) were dissolved completely in 50 mL of ethylene glycol (EG). Then KI or NaBr were added with the equivalent molar ratio and stirred for 30 min to form the fine suspension at room temperature (25℃). Thereafter, the suspension was transferred into the 100 mL Teflon-lined stainless steel autoclave. Then 30 ml EG were added into the autoclave, which was heated at 160 ℃ for 12 h. Subsequently, the autoclave was cooled to room temperature gradually. Finally, the precipitates were filtered and washed with ethanol and deionized water for several times, and dried at 70 ℃ for 6h.

Characterization

The as-prepared powder catalysts were first characterized by X-ray diffraction (XRD) using a D/max-2550 PC diffractometer (Rigaku, Japan) with radiation of Cu-Kα at an accelerating voltage of 40kV and a current of 200 mA. The morphologies of the catalysts were observed with S-4800 field emission scanning electron microscopy (SEM, HITACHI, Japan) and high-resolution transmission electron microscopy (HRTEM). The content of elements in the BiOI/BiOBr composite was determined by SEM-EDS thermal field emission scanning electron microscopy (IE 300 X, Oxford). Nitrogen adsorption-desorption isotherms were measured using a NOVA 4000e sorption instrument (Chrome, Quanta). The absorption edge of the catalysts was examined by a UV–vis spectrophotometer (Lambda 35, PerkinElmer, USA) equipped with an integrating sphere to record the diffuse reflectance spectra (DRS) by using a reflectance standard of $BaSO_4$.

Photocatalytic bacteriostasis **of *Escherichia coli* under visible light**

E.coli, a Gram-negative bacterium, was used as model bacteria in this study. It was incubated in Nutrient Broth (NB) solution at 37℃ and agitated at 170 rpm for 18 h. The cultures were then washed with sterilized saline (0.9% NaCl) solution by centrifugation for 5 min, and then the cell pellet was re-suspended in sterilized saline solution. All glassware used in the experiments was autoclaved at 121 ℃ for 20 min to ensure sterility before use. The experiments of photocatalytic bacteriostasis were conducted by using a 500 W Xenon lamp with a 420 nm cut-off filter. The light was then focused onto a quartz tube containing a suspension of bacterial cells and photocatalyst. The reaction mixture was stirred with a magnetic stirrer throughout the experiment. The final cell density and photocatalyst concentration were adjusted to about 2×10^5 colony forming units per milliliter (cfu/mL) and 1 g/L, respectively. Before irradiation, the mixture was magnetically stirred for 30 min in dark to ensure the establishment of an adsorption/desorption equilibrium between the photocatalyst and bacterial cells. At the certain time intervals, 1 mL of the reaction solution was sampled and immediately diluted 10-fold serially with sterilized saline. 0.1 mL of the diluted sample was then immediately spread on a nutrient agar medium and incubated at 37 ℃ for 24 h to determine the number of viable cells (in cfu). For comparison, a bacterial suspension without photocatalyst was irradiated as a control, and the reaction mixture without visible light irradiation was used as a dark control. The survival ratio of E.coli was determined by the ratio of N_t/N_0, where N_0 and N_t are the numbers of cfu at the initial and each following time interval, respectively. The release of K^+ from the disinfected bacteria was an index to the destruction level of bacteria. To investigate K^+ leakage from the bacterial cells during the photocatalytic inactivation process, the suspension before and after inactivation treatment was collected and filtered through a Millipore filter (pore size of 0.45 μm). After filtration, the K^+ concentration in the resulting clear solution was measured by inductively coupled plasma optical emission spectrometry (ICP-OES) (Leeman Prodigy, USA). All the previous experiments were performed in triplicate.

Preparation of *E.coli* for TEM

The mixture of the catalyst and E.coli at different reaction time was collected and centrifuged down to pellets. In order to maintain the original shape of the cell, the bacteria pellets were prefixed in 2.5% glutaraldehyde at 4 ℃ for 4 h, and then washed twice with 0.1 M phosphate buffer (PBS) (pH 7.2). For electron microscopy observation, biological samples with low e-scattering ability were usually colored by heavy metals to increase the contrast of samples. The specimens were mixed with 2% $Na_3[P(W_3O_{10})_4]$ aqueous solution with a volume ratio 1:1. Then mixing suspensions were dropped onto copper grids and dried naturally. Finally, the obtained dry copper grids were examined by a JEM-2100 transmission electron microscope (JEOL Ltd., Tokyo, Japan).

Results and discussion

Material characterization

The typical XRD patterns of the pure BiOI, BiOBr and the BiOI/BiOBr composite were given in Fig. 1. It indicates that all the catalysts were well crystallized and all the diffraction peaks can be indexed to the tetragonal tetragonal BiOI (JCPDS 09-0393) and BiOBr (JCPDS 10-0445), respectively. No characteristic peaks of other crystalline impurities were observed. In addition, according to the previous reports, with increasing amounts of BiOBr in the BiOI/BiOBr composites, the intensities of the diffraction peaks of BiOBr gradually increased and became broader, whereas the diffraction peaks of BiOI simultaneously decreased. Interestingly, the diffraction peaks shifted to larger angles as the BiOBr amounts increased. All XRD patterns revealed a strong preference to grow along the (102) and (110) directions. However, comparison with the JCPDS standard revealed that the peak of the (102) plane was suppressed compared to the (110) plane, indicating that the crystals grew isotropic ally along the (110) plane [16]. According to the previous reports [26, 27], this selective absorption of PVP in particular planes contributed to the facet-controlled

fabrication efficiency of nanostructures. This specific crystal plane exposition may play a role in photoexcitation [28].

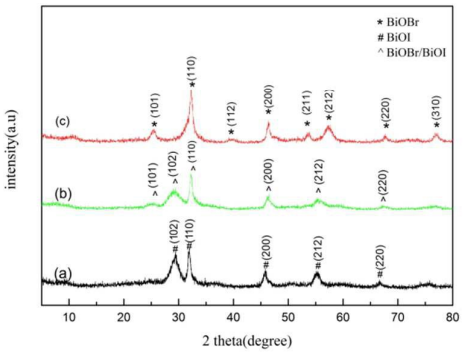

Fig.1 XRD patterns of (a) BiOI, (b) BiOI/BiOBr composites with 50% BiOBr, (c) BiOBr

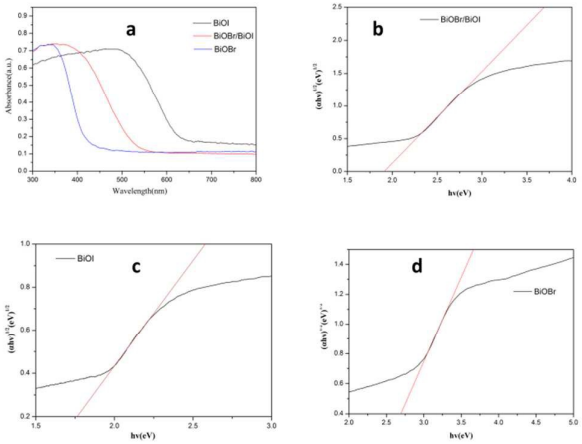

Fig.2 (a) UV–vis diffuse reflection spectra; (b-d) plots of $(\alpha hv)^{1/2}$ vs. photo energy.

One of the critical factors determining the photocatalytic performance is the energy band structure feature of the as-prepared BiOI/BiOBr composites. Fig.2 (a) reveals that as-prepared samples exhibit strong absorptions in the visible light region. At about 435nm and 675 nm, BiOBr and BiOI both show the absorption edges in the visible light region, respectively, which is similar to other reported previously [29]. The band gap energy can be calculated by the formula [9, 18]:

$$\alpha hv = A(hv - E_g)^{n/2} \quad (1)$$

Where a, v, A, and Eg was absorption coefficient, light frequency, a constant and band gap, respectively. n depends on the characteristics of the transition in a semiconductor. With respect to BiOX (X=Br, I), the value of n is 4 for the indirect transition [30]. Thus, the plot of (ahv) $^{1/2}$ versus the photon energy (hv) would estimate approximate bandgaps of the catalysts as shown in Fig. 2b-d. The bandgap energies of the samples were estimated to be 2.68eV, 1.90 eV and 1.76 eV, corresponding to BiOBr, BiOI/BiOBr and BiOI, respectively. Thus, it is indicated that the better optical absorption in visible light range is an essential condition to perform photocatalytic reaction under visible light irradiation. The morphology of the samples was investigated by SEM. As shown in Fig.3 (a-c), it can be seen clearly that the catalysts were consisted of interwoven nanoplates and appeared as three-dimensional hierarchical microspheres with diameters in the range of 1-5 μm: pure BiOI of 2-4 μm, pure BiOBr of 1-3 μm and the BiOI/BiOBr composites reduced to 1-2 μm. The microspheres were composed of a great many irregular nanoplates to form the polyporous surface. Though the sizes of the microspheres are non-uniform, the gaps between neighboring nanoplates were observed to be larger. It was found that EG played a significant role in the formation process of the hierarchical microspheres in the reaction system [7]. The rough surface of the microspheres confers high specific surface area, surface-to-volume ratio and abundant transport paths for small organic molecules, which are considered towards photo catalysis [31]. EDS pattern of BiOI/BiOBr composite is shown in Fig.3d, which indicates the presence of Bi, Br, I, and O in the catalysts, which generally conforms to the previous XRD analysis. The specific BET surface areas (S_{BET}) and pore structure (V_{BJH}) of the prepared samples were investigated using adsorption–desorption measurements, which is shown in Table 1.

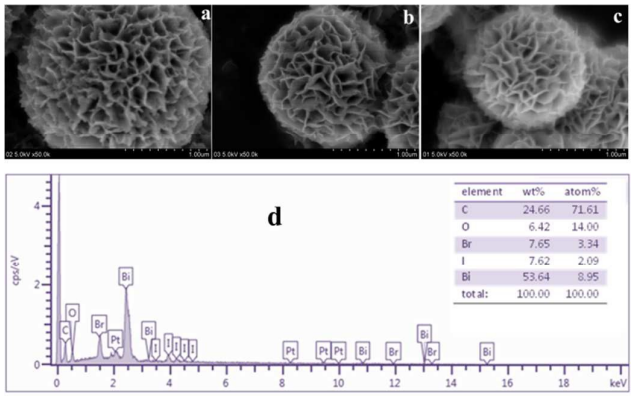

Fig.3 SEM images of BiOI (a), BiOBr(b), BiOI/BiOBr (c) and EDS spectrum of BiOI/BiOBr composite (d). Inset: the table of element integrating data.

Table **1** Specific BET surface areas, pore volumes for samples

Samples	S_{BET} (m^2/g)	V_{BJH} (cm^3/g)
BiOI/BiOBr	24.32	0.0901
BiOI	40.82	0.1167
BiOBr	36.36	0.1354

HRTEM is an efficient and widely used characterization means of heterojunction [32, 33]. Fig. 4 shows TEM and HRTEM images of the BiOI/BiOBr. It can be observed in Fig. 4b, two crystals of BiOBr and BiOI are tightly interconnected. The lattice fringe spacing of 0.304 nm corresponds to the (1 0 2) crystallographic plane of BiOI and the lattice fringe spacing of 0.279 nm matches the (1 1 0) plane of BiOBr, which are in good accordance with the results of the XRD analysis. The HRTEM

analysis further confirms that the heterostructures of BiOBr and BiOI have been formed in the samples.

Photocatalytic activities for *E.coli* bacteriostasis

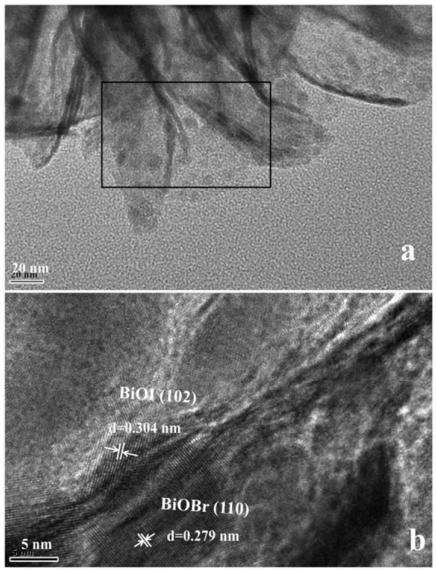

Fig.4 images of the BiOI/BiOBr (a) TEM and (b) HRTEM

The bacteriostatic activity of the BiOI/BiOBr was evaluated by the killing effect of *E.coli* in water under visible light irradiation,

which were calculated by the decrease of the colony number formed on an agar plate. Fig.5 shows the photocatalytic bacteriostatic efficiencies of *E.coli* over different photocatalysts. As is shown in Fig.5, a blank experiment under visible light irradiation in the absence of the photocatalyst showed that the photolysis of *E.coli* was negligible. Neither visible light without the photocatalyst nor BiOI/BiOBr in the dark showed any bacteriostatic effects on *E.coli*, indicating that the photocatalyst itself is not toxic to *E.coli*. Thus, the bacteriostatic effect on *E.coli* is ascribed to the photocatalytic reaction of the samples under visible light irradiation. From the figure, it indicated that pure BiOBr and BiOI showed some visible light bacteriostatic activity, and the effect of BiOI was better than BiOBr for the same time. More interesting, the photocatalytic activity of the composite of BiOI/BiOBr was obviously enhanced as compared to the pure BiOI. With the visible light irradiation on BiOI/BiOBr, about 90% of *E.coli* was almost killed after 12 h irradiation, whereas only about 70% and 60% of E.coli was killed after 12 h in the present of BiOI and BiOBr under the same condition, respectively. The results demonstrate that photocatalytic bacteriostatic activity of the composites could be greatly enhanced by in situ formation of BiOI/BiOBr heterostructures on the surface of BiOBr or BiOI.

According to the previous study, there are two main mechanisms presented to explain the photocatalytic inactivation of pathogenic bacteria. The first putative killing mechanism proposed by Matsunaga et al. implies an oxidation of the intracellular coenzyme A (*Co*A), which inhibits the cell respiration and subsequently causes cell death as a result of a direct contact between the photocatalysts and the target cells [4]. The second killing mode suggests that bacterial death is caused by a significant disorder in the cell permeability and by the decomposition of the cell walls [34]. To investigate the

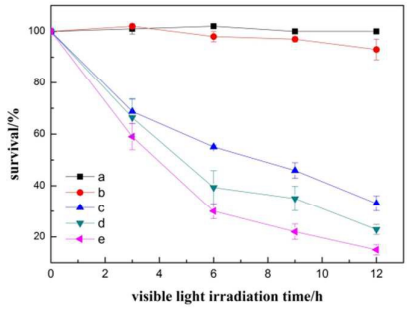

Fig.5 Survival ratio of E.coli over the various samples (0.5mg/mL) under visible-light irradiation (a) BiOI/BiOBr in dark; (b) no catalyst; (c) BiOBr; (d) BiOI; (e) BiOI/BiOBr

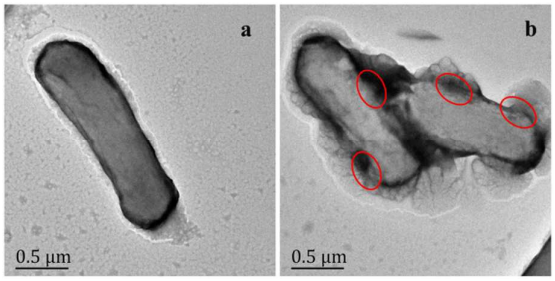

Fig.6 TEM images of E.coli before and after photocatalytic bacteriostasis. (a)Before irradiation (b) After irradiation for 12h

cell destruction, the morphology of *E.coli* before and after photocatalytic bacteriostatic experiment was observed by TEM microscopy (Fig. 6). Fig. 6a is a representative TEM image of untreated *E. coli* that had a well-defined cell wall and evenly colored interior. After the damage of *E. coli* over the BiOI/BiOBr under illumination for 12h, the *E. coli* cells were fragmented. The Fig.6b indicates that the cell membrane could be destroyed and the intracellular content had leaked out. TEM further indicates that the cell membrane were destroyed.

The bacteriostatic action was further confirmed by the measurement of K^+, which played a role in the regulation of polysome content and protein synthesis of the bacteria cells. To investigate the permeability of the cell membrane, the measurement of K^+ leakage from the inactive *E.coli* was carried out by ICP-OES before and after every experiment respectively (Fig. 7). The K^+ leakage during different bacteriostatic periods was shown in Fig. 7.

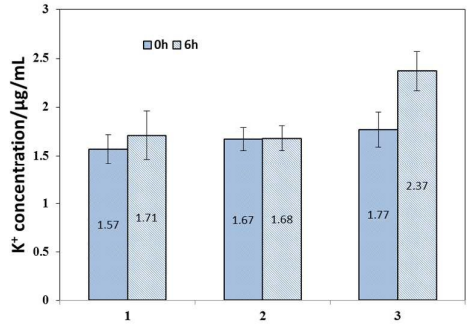

Fig.7 Potassium ion (K^+) leakage from E. coli under different conditions: (1) visible light with no catalyst (2) the catalyst BiOI/BiOBr in dark and (3) the catalyst BiOI/BiOBr with visible ligh

With catalysts in the dark or no catalysts in visible light, the K^+ leakage from *E.coli* cells was almost the same or only a slight increase with the time prolonging. Contrarily, K^+ leakage increased notably with the catalysts under visible light irradiation. However, the number of dead bacteria is not proportional to the detected K^+ concentrations. The membrane of partial bacteria may not be damaged badly, especially the cytoplasmic membrane was still unspoiled and did not leak out the K^+ , but the cells had already lost their viability, which cannot propagate into a visible colony anymore [35, 36]. Therefore, the K^+ concentrations and the number of dead bacteria are not proportional.

Photocatalytic bacteriostatic mechanism

To investigate the mechanism of the bacteriostasis, the band edge positions of BiOI and BiOBr can be determined by the following formula:

$$E_{CB} = x - E^e - \frac{1}{2}E_g \quad (2)$$

$$E_{VB} = x - E^e + \frac{1}{2}E_g \quad (3)$$

where E_g is the bandgap of the semiconductor. E^e is the energy of free electrons on the hydrogen scale ca. 4.5 eV. x is the electronegativity of the semiconductor, expressed as the geometric mean of the absolute electronegativity of the constituent atoms, which is defined as the arithmetic mean of the atomic electron affinity and the first ionization energy [37]. The bandgap energies of BiOI and BiOBr are 1.76 eV and 2.68 eV, as the results derived from UV–vis diffuse reflectance (Fig. 2). Given the equation above, the top of valance band (E_{VB}) and bottom of the conduction band (E_{CB}) of BiOI were calculated to be 2.48 and 0.72 eV. The E_{VB} and E_{CB} of BiOBr were calculated to be 3.17and 0.49 eV, respectively. Therefore, the schematic band energy levels and charge transfer processes of the BiOI/BiOBr composites can be depicted as Fig. 8.

As well known, h^+, •OH and e^- are often proposed to be the reactive species responsible for the photocatalytic disinfection. To understand which reactive species played an important role in BiOI/BiOBr photocatalytic bacteriostasis under VL irradiation, a series of scavenger experiments were carried out by adding individual scavenger to the photocatalytic reaction system. In the experiments, 0.5 mM isopropanol , 0.5 mM sodium oxalate and 0.05 mM Cr(VI) were used to remove •OH, h^+ and e–, respectively. As reported, all the scavengers had no toxic effect on *E.coli* at this level of concentrations [14]. As shown in Fig.9, with the addition of isopropanol or Cr(VI), about half of *E.coli* could be killed in 6 h. However, only about 30% of *E.coli* was killed at the presence of sodium oxalate. Hence, comparing with •OH and e^-,the generated active h^+ is the biggest driving force for the photocatalytic bacteriostatic activity of *E.coli* in the experiments.

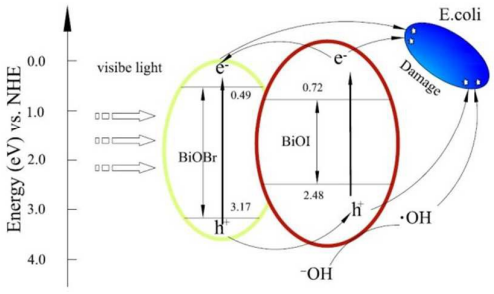

Fig.8 Schematic illustration for energy bands structure, electron–hole separation and transportation for the BiOI/BiOBr composite

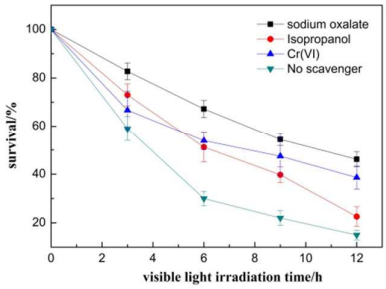

Fig.9 Survival ratio of E.coli over the various scavengers

Conclusions

The BiOI/BiOBr composite with 3D hierarchical microsphere structures for photocatalytic bacteriostatic activity of *E.coli* under visible light irradiation was successfully synthesized via a one-pot solvothermal method. It exhibited largely enhanced photocatalytic inactivation of *E.coli* under visible light irradiation in water than the single BiOI and BiOBr, predominantly attributed to the efficient electron–hole separations at the interfaces of the two components, which is the heterojunction structure. The determination of cell structure destruction by TEM microscopy and the released K^+ further confirmed that the cell membranes of *E.coli* were ruptured in the photocatalytic bacteriostatic activity. In addition, h^+ radicals could be the biggest active species during the photocatalytic bacteriostatic process.

Acknowledgements

This work was supported by the National Natural Science Foundation of China (No.21477018, 21007010) and the fundamental research funds for the central universities (No.15D111323).

References

1. D. Schoenen, Role of disinfection in suppressing the spread of pathogens with drinking water: possibilities and limitations, *Water Res.*, 2002, **36**, 3874-3888.
2. L. M. Fry, J. R. Mihelcic and D. W. Watkins, Water and nonwater-related challenges of achieving global

sanitation coverage, *Environ. Sci. Technol.*, 2008, **42**, 4298-4304.

3. M. G. Muellner, E. D. Wagner, K. McCalla, S. D. Richardson, Y. T. Woo and M. J. Plewa, Haloacetonitriles vs. regulated haloacetic acids: Are nitrogen-containing DBPs more toxic, *Environ. Sci. Technol.*, 2007, **41**, 645-651.
4. T. Matsunaga, R. Tomoda, T. Nakajima and H. Wake, Photoelectrochemical sterilization of microbial-cells by semiconductor powders, *FEMS Microbiol. Lett.*, 1985, **29**, 211-214.
5. L. F. Zhang, T. Kanki, N. Sano and A. Toyoda, Development of TiO_2 photocatalyst reaction for water purification, *Sep. Purif. Technol.*, 2003, **31**, 105-110.
6. J. Henle, P. Simon, A. Frenzel, S. Scholz and S. Kaskel, Nanosized BiOX (X = Cl, Br, I) particles synthesized in reverse microemulsions, *Chem. Mater.*, 2007, **19**, 366-373.
7. X. Zhang, Z. Ai, F. Jia and L. Zhang, Generalized one-pot synthesis, characterization, and photocatalytic activity of hierarchical BiOX (X = Cl, Br, I) nanoplate microspheres, *J. Phys. Chem. C*, 2008, **112**, 747-753.
8. J. Xia, S. Yin, H. Li, H. Xu, Y. Yan and Q. Zhang, Self-Assembly and Enhanced Photocatalytic Properties of BiOI Hollow Microspheres via a Reactable Ionic Liquid, *Langmuir*, 2011, **27**, 1200-1206.
9. Y. Li, J. Wang, H. Yao, L. Dang and Z. Li, Efficient decomposition of organic compounds and reaction mechanism with BiOI photocatalyst under visible light irradiation, *J. Mol. Catal. A-Chem,* 2011, **334**, 116-122.
10. H. G. Kim, D. W. Hwang and J. S. Lee, An undoped, single-phase oxide photocatalyst working under visible light, *J. Am. Chem. Soc.*, 2004, **126**, 8912-8913.
11. L. Zhang, H. Wang, Z. Chen, P. K. Wong and J. Liu, Bi2WO6 micro/nano-structures: Synthesis, modifications and visible-light-driven photocatalytic applications, *Appl. Catal. B-Environ.*, 2011, **106**, 1-13.
12. C. Hu, X. Hu, J. Guo and J. Qu, Efficient destruction of pathogenic bacteria with $NiO/SrBi_2O_4$ under visible light irradiation, *Environ. Sci. Technol.*, 2006, **40**, 5508-5513.
13. W. Wang, Y. Yu, T. An, G. Li, H. Y. Yip, J. C. Yu and P. K. Wong, Visible-Light-Driven Photocatalytic Inactivation of E. coli K-12 by Bismuth Vanadate Nanotubes: Bactericidal Performance and Mechanism, *Environ. Sci. Technol.*, 2012, **46**, 4599-4606.
14. H. Gan, G. Zhang and H. Huang, Enhanced visible-light-driven photocatalytic inactivation of Escherichia coli by $Bi_2O_2CO_3/Bi_3NbO_7$ composites, *J. Hazard. Mater.*, 2013, **250**, 131-137.
15. G. Liu, L. Wang, H. G. Yang, H.-M. Cheng and G. Q. Lu, Titania-based photocatalysts-crystal growth, doping and heterostructuring, *J. Mater. Chem.*, 2010, **20**, 831-843.
16. L. Lin, M. Huang, L. Long, Z. Sun, W. Zheng and D. Chen, Fabrication of a three-dimensional BiOBr/BiOI photocatalyst with enhanced visible light photocatalytic performance, *Ceram. Int.*, 2014, **40**, 11493-11501.
17. X. Xiao, R. Hao, M. Liang, X. Zuo, J. Nan, L. Li and W. Zhang, One-pot solvothermal synthesis of three-dimensional (3D) BiOI/BiOCl composites with enhanced visible-light photocatalytic activities for the degradation of bisphenol-A, *J. Hazard. Mater.*, 2012, **233**, 122-130.
18. H. Cheng, B. Huang, Y. Dai, X. Qin and X. Zhang, One-Step Synthesis of the Nanostructured AgI/BiOI Composites with Highly Enhanced Visible-Light Photocatalytic Performances, *Langmuir*, 2010, **26**, 6618-6624.
19. S. Shamaila, A. K. L. Sajjad, F. Chen and J. Zhang, WO_3/BiOCl, a novel heterojunction as visible light photocatalyst, *J. Colloid Interface Sci.*, 2011, **356**, 465-472.
20. D. He, L. Wang, D. Xu, J. Zhai, D. Wang and T. Xie, Investigation of Photocatalytic Activities over $Bi_2WO_6/ZnWO_4$ Composite under UV Light and Its Photoinduced Charge Transfer Properties, *ACS Appl. Mater. Interfaces*, 2011, **3**, 3167-3171.
21. F. Dong, Y. Sun, M. Fu, Z. Wu and S. C. Lee, Room temperature synthesis and highly enhanced visible light photocatalytic activity of porous BiOI/BiOCl composites nanoplates microflowers, *J. Hazard. Mater.*, 2012, **219**, 26-34.
22. F. Dong, T. Xiong, Y. Sun, Y. Zhang and Y. Zhou, Controlling interfacial contact and exposed facets for enhancing photocatalysis via 2D-2D heterostructures, *Chem. C.*, 2015, **51**, 8249-8252.
23. J. L. Liang, C. Shan, X. Zhang and M. P. Tong, Bactericidal mechanism of BiOI-AgI under visible light irradiation, *Chem. Eng. J.*, 2015, **279**, 277-285.
24. W.-K. Chang, D.-S. Sun, H. Chan, P.-T. Huang, W.-S. Wu, C.-H. Lin, Y.-H. Tseng, Y.-H. Cheng, C.-C. Tseng and H.-H. Chang, Visible light-responsive core-shell structured In_2O_3@$CaIn_2O_4$ photocatalyst with superior bactericidal properties and biocompatibility, *Nanomed-Nanotechnol,* 2012, **8**, 609-617.
25. N. Talebian, M. R. Nilforoushan and E. B. Zargar, Enhanced antibacterial performance of hybrid semiconductor nanomaterials: ZnO/SnO_2 nanocomposite thin films, *Appl. Surf. Sci.*, 2011, **258**, 547-555.
26. X. Shi, X. Chen, X. Chen, S. Zhou, S. Lou, Y. Wang and L. Yuan, PVP assisted hydrothermal synthesis of BiOBr hierarchical nanostructures and high photocatalytic capacity, *Chem. Eng. J.*, 2013, **222**, 120-127.
27. J. Xia, S. Yin, H. Li, H. Xu, L. Xu and Q. Zhang, Enhanced photocatalytic activity of bismuth oxyiodine (BiOI) porous microspheres synthesized via reactable ionic liquid-assisted solvothermal method, *Colloids Surf. A Physicochem Eng. Asp.,* 2011, **387**, 23-28.
28. J. Jiang, K. Zhao, X. Xiao and L. Zhang, Synthesis and Facet-Dependent Photoreactivity of BiOCl Single-Crystalline Nanosheets, *J. Am. Chem. Soc.*, 2012, **134**, 4473-4476.
29. K. Ren, J. Liu, J. Liang, K. Zhang, X. Zheng, H. Luo, Y. Huang, P. Liu and X. Yu, Synthesis of the bismuth oxyhalide solid solutions with tunable band gap and photocatalytic activities, *Dalton T.,* 2013, **42**, 9706-9712.
30. W. L. Huang and Q. Zhu, DFT Calculations on the Electronic Structures of BiOX (X = F, Cl, Br, I) Photocatalysts With and Without Semicore Bi 5d States, *J. Comput. Chem.*, 2009, **30**, 183-190.
31. J. Li, G. Lu, Y. Wang, Y. Guo and Y. Guo, A high activity photocatalyst of hierarchical 3D flowerlike ZnO microspheres: Synthesis, characterization and catalytic activity, *J. Colloid Interface Sci.*, 2012, **377**, 191-196.
32. H. G. Kim, P. H. Borse, J. S. Jang, E. D. Jeong, O.-S. Jung, Y. J. Suh and J. S. Lee, Fabrication of $CaFe_2O_4/MgFe_2O_4$ bulk heterojunction for enhanced visible light photocatalysis, *Chem. Commun.*, 2009, 5889-5891.
33. J. Jiang, X. Zhang, P. Sun and L. Zhang, ZnO/BiOI Heterostructures: Photoinduced Charge-Transfer Property

and Enhanced Visible-Light Photocatalytic Activity, *J. Phys. Chem. C*, 2011, **115**, 20555-20564.

34. T. Saito, T. Iwase, J. Horie and T. Morioka, Mode of photocatalytic bactericadal action of powdered semiconductor TIO_2 on mutans streptococcl, *J. Photoch. Photobio. B.*, 1992, **14**, 369-379.
35. Y. Li, M. Ma, X. Wang and X. Wang, Inactivated properties of activated carbon-supported TiO_2 nanoparticles for bacteria and kinetic study, *J. Environ. Sci.-CN*, 2008, **20**, 1527-1533.
36. J. Ren, W. Wang, L. Zhang, J. Chang and S. Hu, Photocatalytic inactivation of bacteria by photocatalyst Bi_2WO_6 under visible light, *Catal. Commun.*, 2009, **10**, 1940-1943.
37. L. Zhu, C. He, Y. Huang, Z. Chen, D. Xia, M. Su, Y. Xionga, S. Li and D. Shu, Enhanced photocatalytic disinfection of E. coli 8099 using Ag/BiOI composite under visible light irradiation, *Sep. Purif. Technol.*, 2012, **91**, 59-66.

Graphical Abstract

Enhanced photocatalytic bacteriostatic activity of *Escherichia coli* using 3D hierarchical microsphere BiOI/BiOBr under visible light irradiation

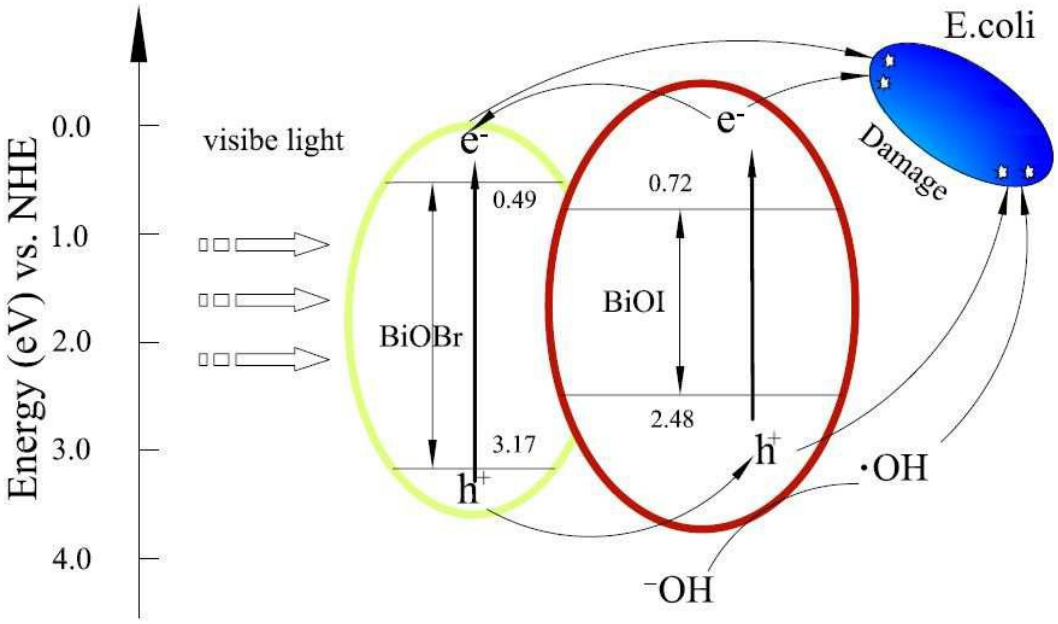

With improved separation efficiency of the photogenerated holes, the BiOI/BiOBr composite exhibited enhanced photocatalytic bacteriostatic activity of *E. coli* as compared to the pure BiOI or BiOBr under visible light irradiation.